

CFD Analysis of a Three Bladed H-Rotor of Vertical Axis Wind Turbine

Y KUMARA SWAMY REDDY¹, A.V. Hari Babu², M SUDHAKAR REDDY³

^{1,2,3}Department of Mechanical Engineering, SVR College of Engineering, Nandyal-518501, INDIA

ABSTRACT - Vertical Axis Wind Turbines (VAWT) are ideal options for small scale generation of electricity from wind. Vertical Axis Wind Turbines are one of the widely developed and are suitable for rooftops and self sustaining light posts. Most research in designing a H-rotor is focused on the experimental side and Computational analysis.

The current thesis explains the wind energy and its advantages in the present situation in world. In this different types wind turbines are explained and out of all those wind turbines how the Vertical Axis Wind Turbines are differed has been explained. These Vertical Axis Wind Turbines are mainly suitable at low wind velocities to produce power from the wind. The first part deals with the modeling of vertical axis wind turbine blades using CFD package CFX. Further the H-Rotor was designed for five H/D ratios and generated models. These models are imported into CFX and generated mesh for the H-Rotor at H/D ratio of turbine. At each H/D ratio of H-Rotor was analysed for three wind velocities of low wind velocities ranging from 2m/s to 6m/s. By the analysis of H-Rotor for five H/D at three wind velocities the power output and power coefficient (C_p) has been determined. The coefficients of power (C_p) values are compared for different low wind velocities at five H/D ratios of H-Rotor. From the results the conclusions can be made for an optimum H/D ratio at different wind velocities for the power generation from the wind.

Keywords -VAWT, H-rotor, CFD, CFX, coefficient of power

1. INTRODUCTION

Horizontal-axis wind turbines (HAWT) get their name from the fact that their axis of rotation is horizontal. They have the main rotor shaft and electrical generator at the top of a tower, and are pointed into the wind. The variability of wind distribution and speed brings up the requirement of a gear system connected to the rotor and the generator. The gear system enables a constant speed of rotation to the generator thus enabling constant frequency generation. Turbine blades are made stiff in order to prevent the blades from being pushed into the tower by high winds. Downwind machines have also been built, as they no longer require a yaw mechanism to keep them facing the wind, and also because in high winds the blades can turn out of the wind thereby increasing drag and coming to a stop. Most of the

HAWT's are upwind as downwind systems cause regular turbulence which may lead to fatigue.

1.2. H-Rotor

The Darrieus rotor is a vertical axis wind turbine (VAWT) provided with two or more blades having an aerodynamic airfoil. The blades are normally bent into a chain line and are connected to the hub at the upper and lower side. However, also Darrieus rotors with straight blades (H-Darrieus) have been developed which therefore have large hubs provided with spokes. The energy is taken from the wind by a component of the lift force L working in the direction of rotation. The same principle is used for a horizontal axis wind turbine (HAWT).



Figure 1.1 H-Rotor

There are also VAWT's for which the power is gained by the difference in drag D of the blade moving in the direction of the wind and the blade moving against the wind. A cup anemometer, used for measuring wind speeds, is an example of such a rotor. There are also VAWT's, like the Savonius rotor, which are working on a combination of lift and drag. One of the advantages of using the lift principle is that much higher power coefficients C_p can be realised than for wind turbines using the drag principle. Another advantage is that the tip speed ratio λ , can be much higher resulting in a much higher rpm for the same rotor diameter and in using much lesser material. Although the Darrieus rotor is working according to the lift principle, the maximum C_p is a lot lower than for a well designed HAWT.

1.3. Power in the Wind

The energy that can be extracted from the wind is directly proportional to the cube of the wind speed. Thus, an understanding of the characteristics of the wind (velocity, direction and variation) is critical to all aspects of wind energy generation, from the identification of suitable sites to predictions of the economic viability of wind farm projects, to the design of wind turbines themselves, all is dependent on characteristics of wind. The most striking characteristic of the wind is its random nature. The wind is highly variable, both geographically and temporally. Moreover this variability exists over a very wide range of scales, both in space and time. This is important because extractable energy from wind varies with the cube of wind velocity. Generally more wind is witnessed on the tops of hills and mountains than in low level areas. Even more locally, wind velocities are altered by obstacles such as trees or buildings. For any location there is variation of wind pattern, wind speed may vary from year to year, also wind distribution will change from decade to decade. These long-term variations are not well understood, and thus make it difficult to make predictions of the economic viability of wind-farm projects. Wind distribution is more predictable over shorter time spans like a year, but on shorter time frame like few days the wind energy is difficult to predict. On the whole, it is important that we understand, the wind carries some energy with it, out of which some part is harnessed by the wind turbine. The kinetic energy of air moving at a velocity can be expressed mathematically as in Eq 1.1.

$$E = \frac{1}{2} m v^2 \quad (1.1)$$

$$P = \frac{dE}{dt} \quad (1.2)$$

The rate of change of kinetic energy of the air flowing at a certain velocity (v) through a certain volume is the power possessed by the moving wind. This is the amount of wind energy passing through cross-section per unit time. At a certain given velocity v ,

$$P = \frac{1}{2} \frac{dm}{dt} v^2 \quad (1.3)$$

The rate of change of mass of the air flowing can be determined in Eq 1.4 as

$$\frac{dm}{dt} = \rho A v \quad (1.4)$$

As substitute Eq 1.4 in Eq 1.3, we get

$$P = \frac{1}{2} \rho A v^3 \quad (1.5)$$

This is the theoretical energy possessed by the wind flowing at a certain velocity v .

The equation tells us that the maximum power available from the wind varies according to the projected area or swept area of the turbine. The swept area place an

important role in increasing the available power. The fraction of free flow wind power that can be extracted by a rotor is called Power Coefficient. Power available in the wind is calculated from the air density, swept area and wind speed. According to Betz's Law, the maximum theoretical power coefficient for any type wind turbine is $16/27$ or 0.593 .

At STP conditions ($T=273^0$ K and $P=101.3$ kPa)

$$P_w = 0.647 \rho A v^3 \quad (1.6)$$

$$P_m = \frac{\frac{16}{27} \times \rho A v^3}{2} \quad (1.7)$$

$$A = D \times H,$$

$$\text{Coefficient of power } C_p = \frac{P_m}{P_w} \quad (1.8)$$

2. LITERATURE

A Ghosh, R.Guptha, A Biswas[1] presented the performances of the two-bladed and three-bladed H-Darrieus turbines through wind tunnel experiments. Both the turbines produced a similar value of maximum aerodynamic torque. The two-bladed turbine had a higher peak C_p of 0.25 compared to about 0.22 for the three-bladed turbine. Gupta et al. [1] experimentally evaluated the C_p of a twisted three-bladed airfoil shaped H-Darrieus turbine made from lightweight aluminium blades for various height-to-diameter (H/D) ratios from 0.85 to 2.2 . The height of the turbine was 20 cm and the blade chords were 5 cm wide. The blades were twisted by 30^0 at the trailing ends to decrease the negative wetted area. There was an optimum H/D ratio at which C_p was the maximum. The maximum C_p of 0.151 was obtained at an H/D ratio of 1.10 .

Md Nahid Pervez and Wael Mohhtar [2] presented about CFD study of Vertical Axis Darrieus Wind Turbine. In this analysis was performed for the NACA4518 airfoil and its performance was observed for low speed wind. A profile of a NACA4518 is shown in figure 1. As the airfoil was a blade of a VAWT, it would be subjected to positive and negative angle of attack. So the angle of attack was varied from $(12^0$ to $+12^0$. And the results are presented. Then a 3D model of an airfoil was simulated. Like the 2D analysis, the results of negative and positive angle of attack are presented. And finally a simplified 3D model of a VAWT with 3 blades was simulated. The airflow structure and other major flow characteristics around the turbine were presented. All of the models of the wind turbine used in the study were done by the CAD software SolidWorks™. The length of the wind turbine was 1.514 m. The chord length was 0.127 m.

Mohmed Jibrin, Ibrahim Abdul Malik[3] presented about the Double Three H-Rotor-Savonius Vertical Axis Wind Turbine has a rotor at which centre is a three bucket Savonius blading separated at 120 degrees without overlap. The recommended diameter of the

central Savonius blade is 30% of the entire rotor diameter. The aspect ratio (H/D) for the H-rotor component is such that $1 \leq H/D \leq 2$. The recommended airfoil shapes for the H-Rotor blade are symmetrical airfoils: NACA 0012, NACA 0015 and NACA 0018. The wind approaches and hits the bucket. The impact is more on the concave bucket facing it and consequently rotates it anti-clockwise. The rotation builds up lift which continues increasing the speed of rotation till the operational speed for optimal efficiency is attained.

R Gupta, S Roy and A Biswas[4] presented about Computational Fluid Dynamics (CFD) analysis of an airfoil shaped two-bladed H-Darrieus rotor using Fluent 6.2 software was performed. Based on the CFD results, a comparative study between experimental and computational works was carried out. The H-Darrieus rotor was 20cm in height, 5cm in chord and twisted with an angle of 30° at the trailing end. The blade material of rotor was Fiberglass Reinforced Plastic (FRP). The experiments were earlier conducted in a subsonic wind tunnel for various height-to-diameter (H/D) ratios. A two dimensional computational modeling was done with the help of Gambit tool using unstructured grid. Realistic boundary conditions were provided for the model to have synchronization with the experimental conditions. Two dimensional steady-state segregated solvers with absolute velocity formulation and cell based grid was considered, and a standard k- ϵ viscous model with standard wall functions was chosen. A first order upwind discretization scheme was adopted for pressure velocity coupling of the flow. The inlet velocities and rotor rotational speeds were taken from the experimental results. From the computational analysis, power coefficient (Cp) and torque coefficient (Ct) values at ten different H/D ratios namely 0.85, 1.0, 1.10, 1.33, 1.54, 1.72, 1.80, 1.92, 2.10 and 2.20 were calculated in order to predict the performances of the twisted H-rotor. The variations of Cp and Ct with tip speed ratios were analyzed and compared with the experimental results. The standard deviations of computational Cp and Ct from experimental Cp and Ct were obtained. From the computational analysis, the highest values of Cp and Ct were obtained at H/D ratios of 1.0 and 1.54 respectively. The deviation of computational Cp from experimental Cp was within $\pm 2.68\%$. The deviation of computational Ct from experimental Ct was within $\pm 3.66\%$.

Sukant Roy, A Biswas and Rajat Gupta [5] presented the H-Darrieus rotor is 20 cm in height, 5 cm in chord, and twisted by an angle of 30° at the trailing end to make it self-starting. Rotor blades are made from Fiberglass Reinforced Plastic (FRP). The FRP used is a composite made from polyvinyl chloride (PVC) type thermoplastic reinforced by fine glass fibres. Blade thickness is 5 mm. The blades of the model have provision for the change of H/D ratio with the help of nuts and bolts. The experiments for the aforementioned H-Darrieus rotor were earlier conducted in an open circuit subsonic wind

tunnel for various H/D ratios namely 0.85, 1.0, 1.33, 1.72 and 2.0. The cross-sectional area of the windtunnel test section was 30 cm x 30 cm, and the length of test section was 3 meters. The air velocity of the wind tunnel was adjustable between 0-35 m/s

3. MODELLING OF H-ROTOR

3.1 Introduction- CFD analysis

As a consequence of the rapid evolution of computational power within the last two decades, the significance of numerical flow simulations in the design of hydraulic machinery has grown to a considerable extent. At present CFD simulations can often replace elaborate experiments due to the fact that even complex geometries and entire machines can be modelled. Separate numerical investigations of single turbo-machinery components are common practice, yet these simulations do not account for interactions between the components which have strong influence on the operational behaviour of the entire machine. Due to these interactions, e.g. between the stationary guide vanes and the rotating runner, the so called rotor-stator interactions the flow in turbo-machines is unsteady and highly turbulent. The investigation of these phenomena requires transient simulations and special numerical treatment with respect to the interface between the components. The approach used in an extruded 2D computational fluid dynamics analysis of the H-Rotor blades. The model used in analysis consists of a stream of air impinging on the blade system.

3.2 CFD analysis – Steps

- 2D geometry
- 2D mesh
- Mesh extrusion
- Boundary conditions
- Interfacing
- Solution monitoring and control
- Post processing results

3.3 MODELLING OF H-ROTOR

The modelling of vertical axis wind turbine blades using CFD package called CFX. Further the H-Rotor was designed for five H/D ratios i.e 1.0,1.33,1.54,1.8 and 2.2.

Specifications of H-Rotor

Table 3.1 Specifications of H-Rotor

S.NO	Description	Value
1	Blade height	0.681m
2	Chord length of each blade	0.13m
3	Blade profile	NACA 4518
4	Number of blades	3
5	Diameter of rotor	0.681m

6	Height of rotor from the ground	15m
7	Number of spokes for each blade	2
8	Diameter of shaft of turbine	13cm

3.4 MODELLING OF H-ROTOR AT H/D=1.0,1.3,1.54,1.8

Now the H-Rotor is modelled by using the specifications of turbine for H/D=1.0

Table 3.2 Input data for design of H-Rotor for H/D

S. No	Description	Value of H/D ratios				
		1.0	1.3	1.54	1.8	2.2
1	H/D Ratio	1.0	1.3	1.54	1.8	2.2
2	Diameter of Turbine	0.681 m	0.681 m	0.681 m	0.681 m	0.681 m
3	Height of Turbine Blades	0.681 m	0.9057 m	0.9057 m	1.2258 m	1.5 m
4	Wind Velocity	3m/s, 4m/s and 5m/s	3m/s, 4m/s and 5m/s	3m/s, 4m/s and 5m/s	3m/s, 4m/s and 5m/s	3m/s, 4m/s and 5m/s

For the above dimensions the H-Rotor is designed and is analysed in CFD CFX. The model and mesh figures are shown as follows.

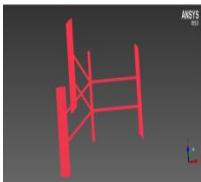


Fig. 3.1 H-Rotor model at H/D=1.0

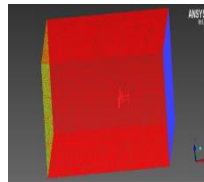


Fig. 3.2 H-Rotor mesh at H/D=1.0

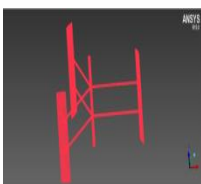


Fig. 3.3 H-Rotor model at H/D=1.33

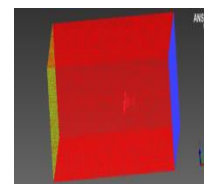


Fig. 3.4 H-Rotor mesh at H/D=1.33



Fig. 3.5 H-Rotor model at H/D=1.54

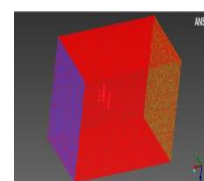


Fig. 3.6 H-Rotor mesh at H/D=1.54



Fig. 3.7 H-Rotor model at H/D=1.8

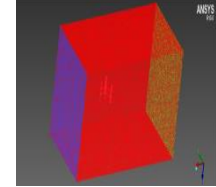


Fig. 3.8 H-Rotor mesh at H/D=1.8



Fig. 3.9 H-Rotor model at H/D=2.2

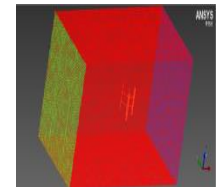


Fig. 3.10 H-Rotor mesh at H/D=2.2

In the mesh generation the tetrahedral type is used. The number of nodes are 270208 and number of elements are 1426818 are obtained.

4. ANALYSIS OF H-ROTOR VERTICAL AXIS WIND TURBINE

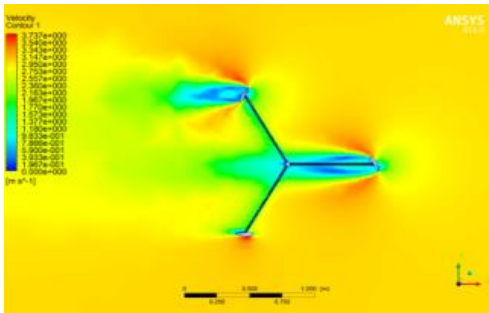
Here the modelled H-Rotor at different H/D ratios is imported into CFX CFD and applied boundary conditions. The solver analyses the H-Rotor at three wind velocities for each H/D ratio.

4.1 ANALYSIS OF H-ROTOR AT H/D=1.0

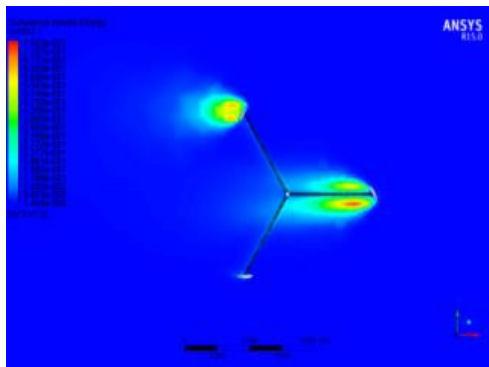
Table 4.1 Power coefficient calculation at 3m/s for H/D=1.0

S.No	Description	Value		
		3m/s,	4m/s,	5m/s,
1	Wind velocity	3m/s,	4m/s,	5m/s,
2	Density of air	1.225kg/m ³	1.225kg/m ³	1.225kg/m ³
3	Swept Area	0.4637m ²	0.4637m ²	0.4637m ²
4	Power in the Wind at 3m/s	7.6694 w	18.1794w	35.5067w
5	Angular Velocity	8.8105rad/s	11.7474rad/s	14.68429rad/s
6	Torque	0.126985 N-m	0.224099 N-m	0.356982 N-m
7	Power Obtained in the Analysis	1.1188w	2.632587 w	5.24202w
8	Power Coefficient Cp	0.1458	0.144811	0.147634

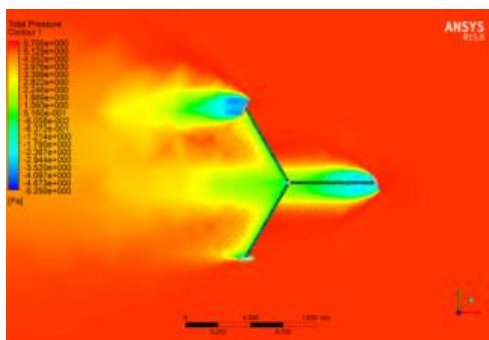
Figure 4.1 Analysis at H/D=1.0 at v=3 m/s



(a) Velocity contour

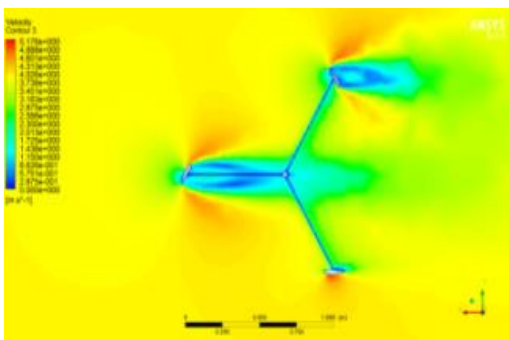


(b) Turbulence kinetic energy

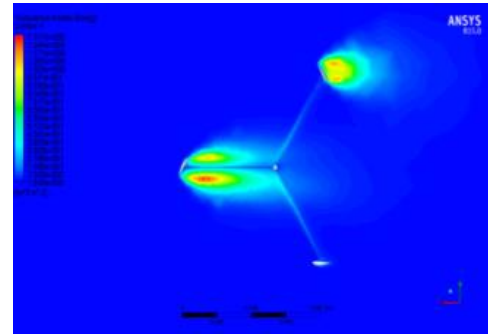


(c) Pressure contour

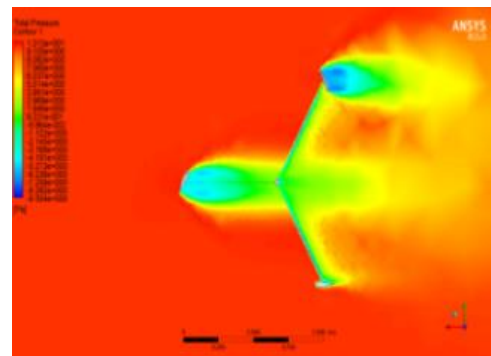
Figure 4.2 Analysis at H/D=1.0 at v=4 m/s



(a) Velocity contour

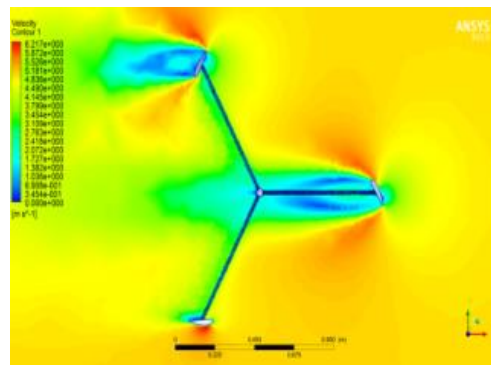


(c) Turbulence kinetic energy

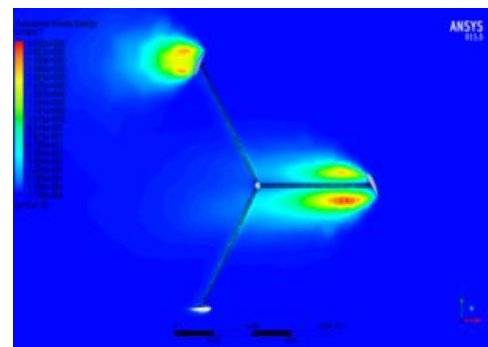


(c) Pressure contour

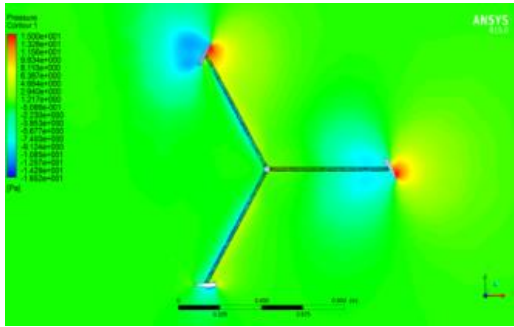
Figure 4.3 Analysis at H/D=1.0 at v=5 m/s



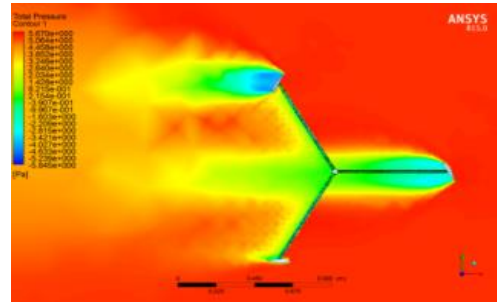
Velocity contour



(b) Turbulence kinetic energy



(c) Pressure contour



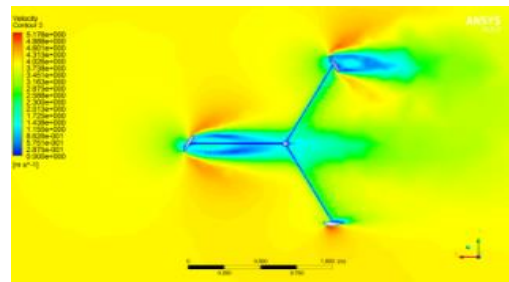
(c) Pressure contour

Figure 4.4 Analysis at H/D=1.0 at v=4 m/s

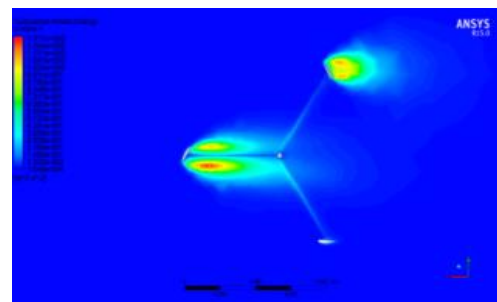
4.2 ANALYSIS OF H-ROTOR AT H/D=1.54

S. No	Description	Value		
1	Wind velocity	3m/s,	4m/s,	5m/s,
2	Density of air	1.225kg/m ³	1.225kg/m ³	1.225kg/m ³
3	Swept Area	0.7141647m ²	0.4637m ²	0.4637m ²
4	Power in the Wind at 3m/s	11.81049w	18.1794w	35.5067w
5	Angular Velocity	8.810573rad/s	11.7474rad/s	14.68429rad/s
6	Torque	0.589524N-m	0.224099N-m	0.356982N-m
7	Power Obtained in the Analysis	5.194044w	2.632587w	5.24202w
8	Power Coefficient Cp	0.439781	0.144811	0.147634

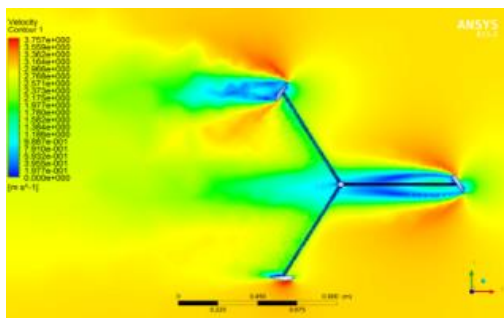
Figure 4.3 Analysis at H/D=1.0 at v=3 m/s



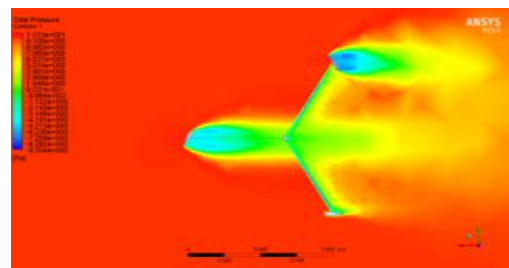
(a) Velocity contour



(b) Turbulence kinetic energy

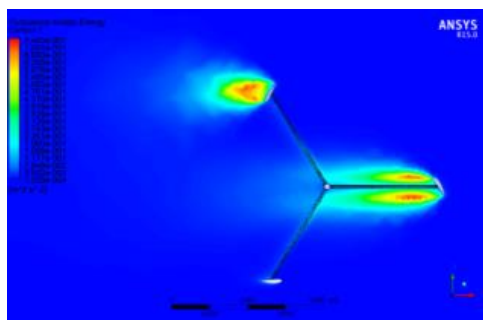


(a) Velocity contour

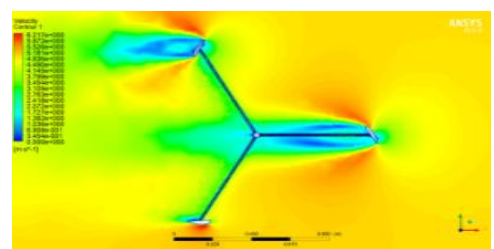


(c) Pressure contour

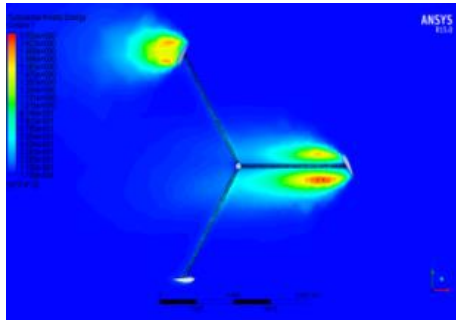
Figure 4.5 Analysis at H/D=1.0 at v=5 m/s



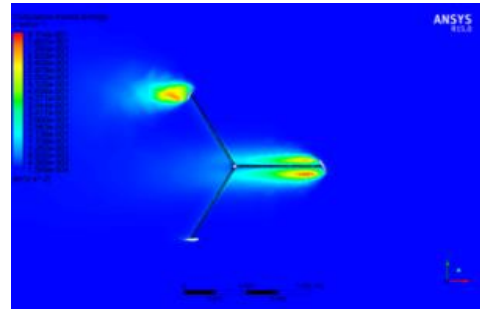
b) Turbulence kinetic energy



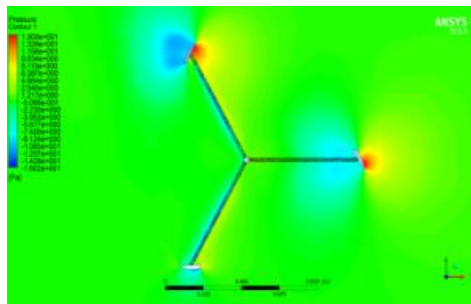
(a) Velocity contour



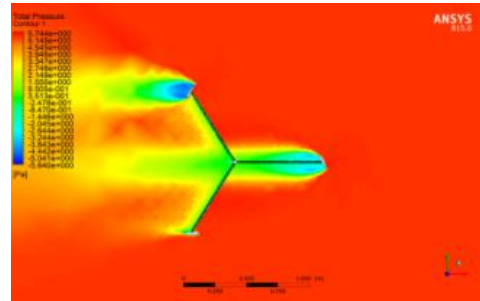
(c) Turbulence kinetic energy



(b) Turbulence kinetic energy



(c) Pressure contour



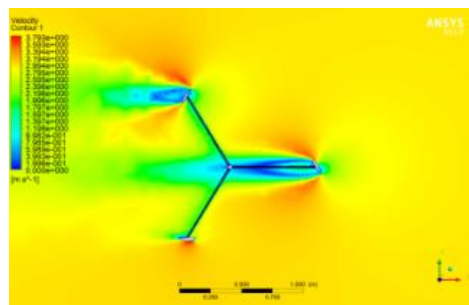
(c) Pressure contour

Figure 4.7 Analysis at H/D=1.0 at v=4 m/s

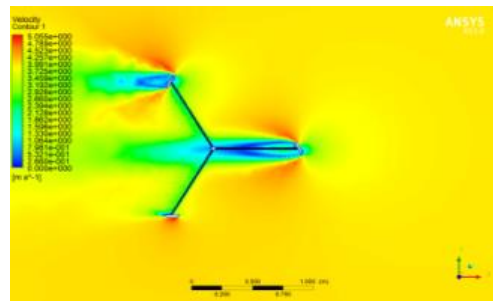
4.3 ANALYSIS OF H-ROTOR AT H/D=2.2

S.No	Description	Value		
		3m/s,	4m/s,	5m/s,
1	Wind velocity	3m/s,	4m/s,	5m/s,
2	Density of air	1.225kg/m ³	1.225kg/m ³	1.225 kg/m ³
3	Swept Area	1.020274 m ²	1.020274m ²	1.020274 m ²
4	Power in the Wind at 3m/s	16.87278 w	39.994748 w	78.1147 w
5	Angular Velocity	8.810573 rad/s	11.74743 rad/s	14.68429 rad/s
6	Torque	0.36545 N-m	0.678824N-m	1.06224 N-m
7	Power Obtained in the Analysis	3.219823 w	7.97443w	15.5982 w
8	Power Coefficient Cp	0.19082	0.19938	0.199683

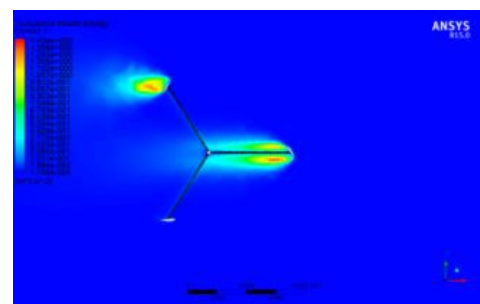
Figure 4.6 Analysis at H/D=1.0 at v=3 m/s



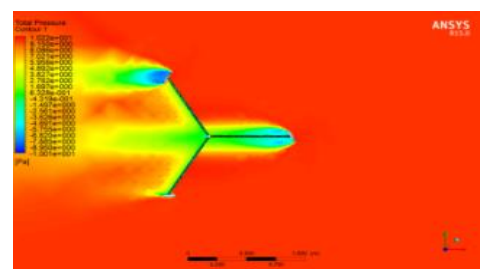
(a) Velocity contour



(a) Velocity contour

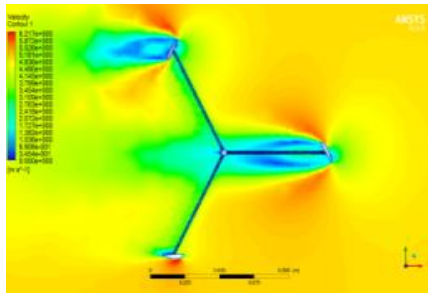


(b) Turbulence kinetic energy

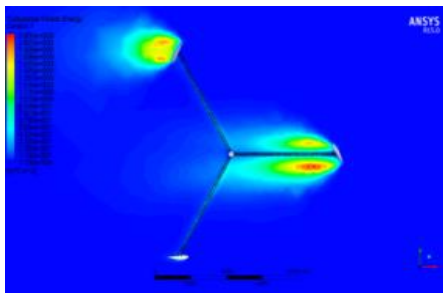


(c) Pressure contour

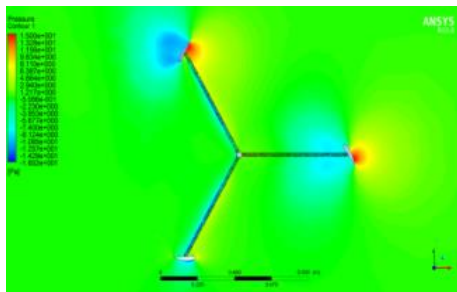
Figure 4.8 Analysis at H/D=1.0 at v=5 m/s



(a) Velocity contour

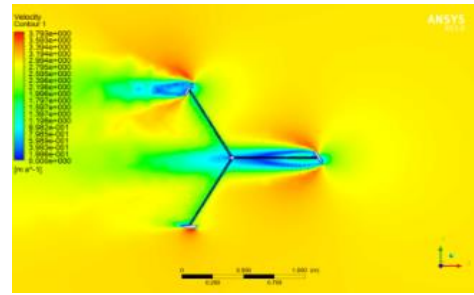


(b) Turbulence kinetic energy

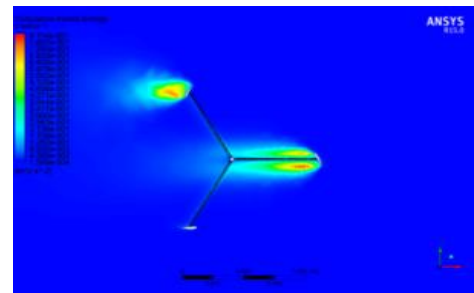


(c) Pressure contour

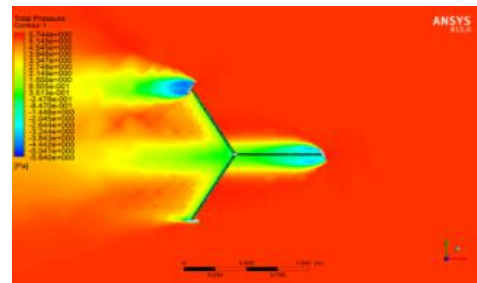
Figure 4.9 Analysis at H/D=1.0 at v=3 m/s



(a) Velocity contour



(b) Turbulence kinetic energy

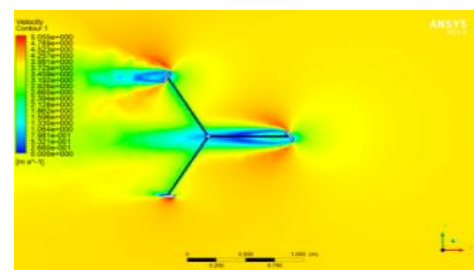


(c) Pressure contour

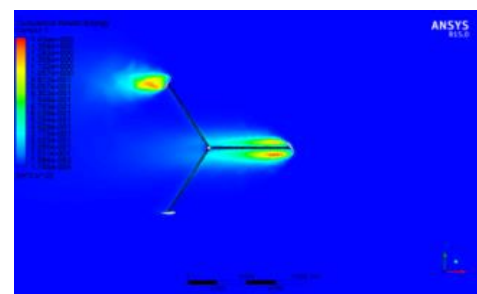
4.4 ANALYSIS OF H-ROTOR AT H/D=1.33

S.No	Description	Value		
1	Wind velocity	3m/s,	4m/s,	5m/s,
2	Density of air	1.225kg/m ³	1.225kg/m ³	1.225kg/m ³
3	Swept Area	0.6168021 m ²	0.616802m ²	0.616802m ²
4	Power in the Wind at 3m/s	10.20036w	24.1786w	47.2239w
5	Angular Velocity	8.810573rad/s	8.810573rad/s	8.810573rad/s
6	Torque	0.29684N-m	0.51256N-m	0.81457N-m
7	Power Obtained in the Analysis	2.61533w	6.02138w	11.96138w
8	Power Coefficient Cp	0.25639	0.249036	0.25329

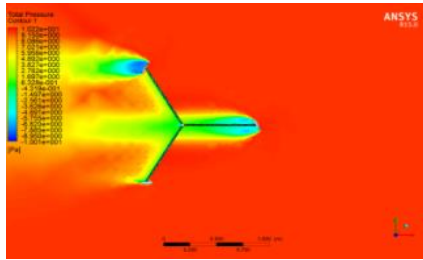
Figure 4.10 Analysis at H/D=1.0 at v=4 m/s



(a) Velocity contour

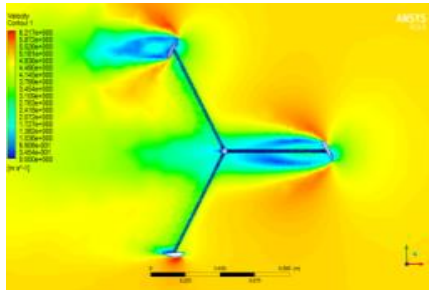


(b) Turbulence kinetic energy

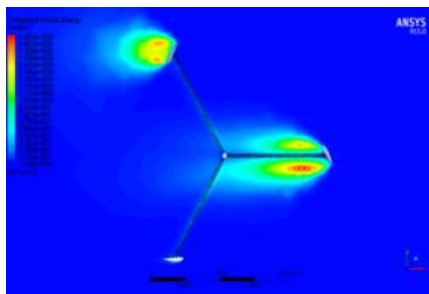


(c) Pressure contour

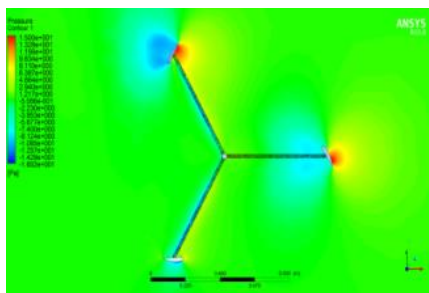
Figure 4.11 Analysis at H/D=1.0 at v=5 m/s



(a) Velocity contour



(b) Turbulence kinetic energy



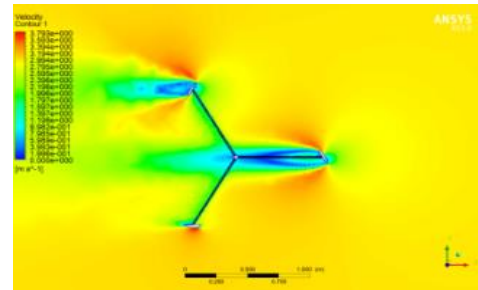
(c) Pressure contour

4.5 ANALYSIS OF H-ROTOR AT H/D=1.8

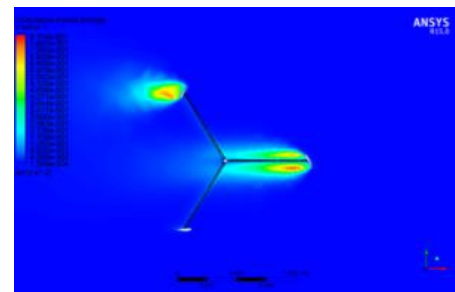
S.No	Description	Value		
		3m/s,	4m/s,	5m/s,
1	Wind velocity	3m/s,	4m/s,	5m/s,
2	Density of air	1.225kg/m ³	1.225kg/m ³	1.225kg/m ³
3	Swept Area	0.8347m ²	0.83476m ²	0.83476m ²
4	Power in the Wind at 3m/s	13.805005w	32.72297w	63.91206w

5	Angular Velocity	8.810573rad/s	8.810573rad/s	8.810573rad/s
6	Torque	0.35698N-m	0.63548N-m	1.03456N-m
7	Power Obtained in the Analysis	3.14519w	7.46525w	15.19177w
8	Power Coefficient Cp	0.2278	0.22813	0.23769

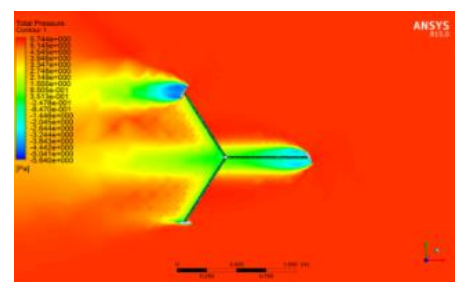
Figure 4.12 Analysis at H/D=1.0 at v=3 m/s



(a) Velocity contour

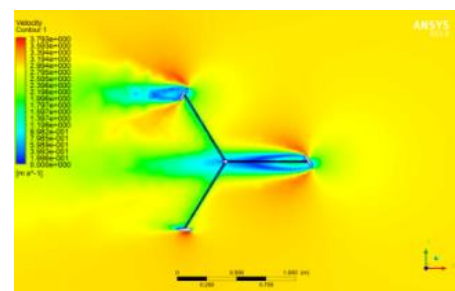


(b) Turbulence kinetic energy

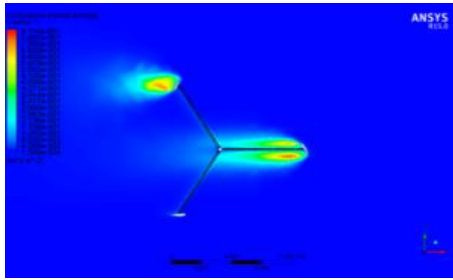


(c) Pressure contour

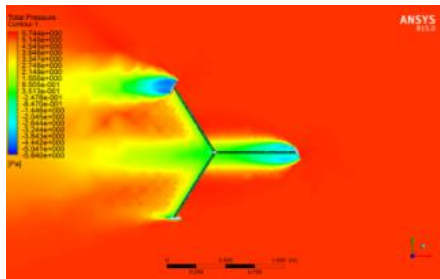
Figure 4.13 Analysis at H/D=1.0 at v=4 m/s



(a) Velocity contour

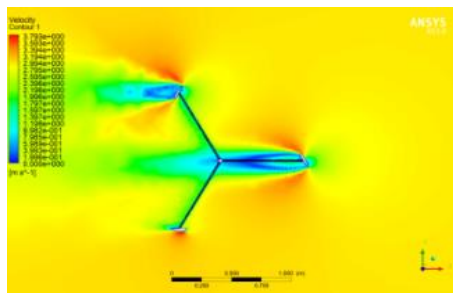


(b) Turbulence kinetic energy

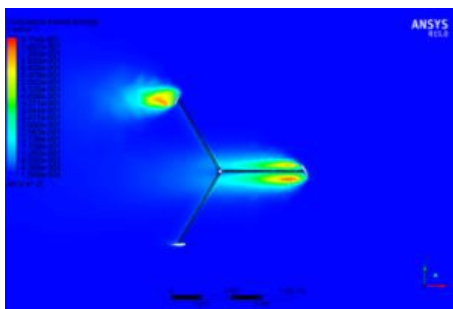


(c) Pressure contour

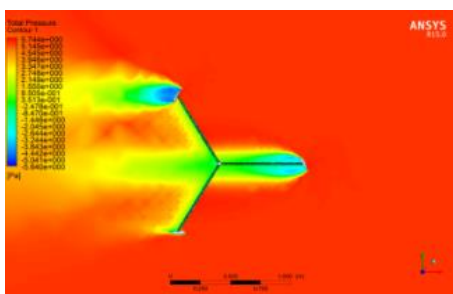
Figure 4.14 Analysis at H/D=1.0 at v=5 m/s



(a) Velocity contour



(b) Turbulence kinetic energy



(c) Pressure contour

5. RESULTS AND DISCUSSIONS

The power coefficient (C_p) is a crucial parameter that determines the performance of H-Rotor. In the analysis of H-Rotor at five H/D ratios for three wind velocities the value of power coefficient is calculated.

The following table describes how the power coefficient is varying with wind velocity and H/D ratio of H-rotor.

Table 5.1 Power coefficient values at wind velocity and H/D ratios.

S. NO	Wind Velocity	C_p at H/D=1.0	C_p at H/D=1.33	C_p at H/D=1.54	C_p at H/D=1.8	C_p at H/D=2.2
1	3	0.1458	0.2563	0.4397	0.2281	0.1908
2	4	0.1448	0.24903	0.4558	0.22813	0.19938
3	5	0.14763	0.25329	0.45117	0.2373	0.199683

The following graph(5.1) explains about the variation of power coefficient C_p at different H/D ratios from H/D ratio 1.0 to 1.54 the value of power coefficient goes on increasing and from 1.54 to 2.2 the value of power coefficient is decreasing. The following graph(5.2) explains about the variation of power coefficient C_p at different H/D ratios from H/D ratio 1.0 to 1.54 the value of power coefficient goes on increasing and from 1.54 to 2.2 the value of power coefficient is decreasing.

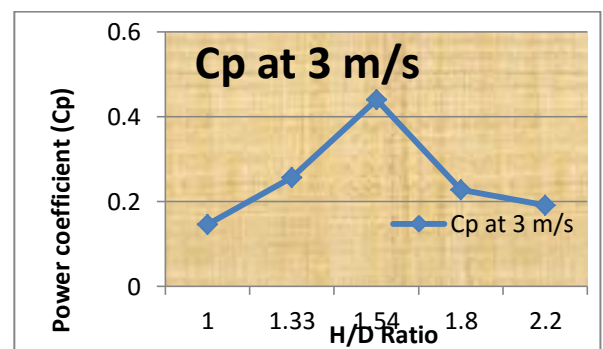


Figure 5.1 Power coefficient Vs H/D ratio at v=3m/s.

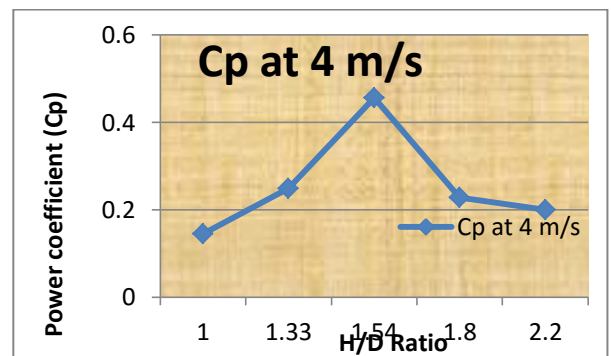


Figure 5.2 Power coefficient Vs H/D ratio at v=3m/s.

The following graph (5.3) explains about the variation of power coefficient C_p at different H/D ratios from H/D ratio 1.0 to 1.54 the value of power coefficient goes on increasing and from 1.54 to 2.2 the value of power coefficient is decreasing. The following graph(5.4) explains about the variation of power coefficient C_p at different H/D ratio from H/D ratio 1.0 to 1.54 the value of power coefficient goes on increasing and from 1.54 to 2.2 the value of power coefficient is decreasing. The variation of power coefficient at three wind velocities shown in the graph. By increasing the wind velocity the power coefficient also increases.

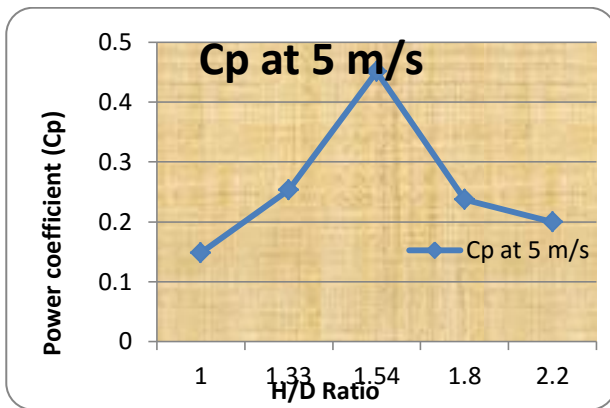


Figure 5.3 Power coefficient Vs H/D ratio at v=3m/s

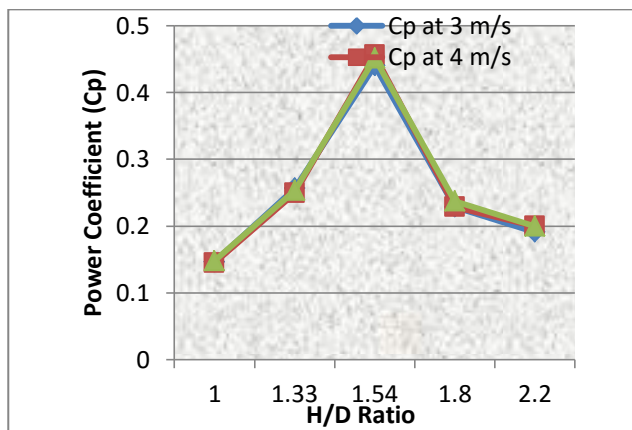


Figure 5.4 Power coefficient Vs H/D ratios at three velocities and comparison.

6. CONCLUSIONS

The following results are concluded from the analysis of H-Rotor of Vertical Axis Wind Turbine.

- The maximum power output was obtained at H/D=1.54 for wind velocity 5m/s.
- In all the five H/D ratios the maximum power output was obtained at H/D=1.54 for all the three wind velocities.

- The power coefficient (C_p) value is maximum at H/D=1.54 for wind velocity 4m/s is obtained.
- The power coefficient (C_p) value is increasing at H/D ratios from 1.0 to 1.54 for three wind velocities.
- The power coefficient (C_p) value is decreasing at H/D ratios from 1.54 to 2.2 for three wind velocities.
- The design of H-Rotor of vertical axis wind turbine is optimised to H/D ratios from 1.0 to 1.54 only. This is because of power coefficient value is decreasing for H/D ratios greater than 1.54.
- Hence it is advisable to design a H-Rotor of three bladed of vertical axis wind turbine of H/D ratios in the range of 1.0 to 1.54.

7. REFERENCES

1. Akshay Pendharkar and Narayan Komerath, "The Low Cost Vertical Axis Wind Turbine" ,Annual Conference of the American Society for Engineering Education, June 2013.
2. Animesh Ghosh, Rajat Gupta, Abhijit Sinha, Agnimitra Biswas, K.K. Sharma , "Some Aspects of Vertical Axis Wind Turbines (VAWTs)-A Review " Volume 9-Number 16-November 2013.
3. Jon DeCoste ,Denise McKay , Brian Robinson, Shaun Whitehead ,Stephen Wrigh , "Vertical Axis Wind Turbine"
4. Md Nahid Pervez and Wael Mokhtar , "CFD Study of a Darreous Vertical Axis Wind Turbine" Grand Valley State University, Grand Rapids, MI 49504.
5. Mohammed U. Jibrin, Ibrahim O. Abdulmalik, Michael C. Amony, Mahdi Makoy and Akonyi N.S, "Evolution of Hybrid VAWT for Low Wind Regime" International Journal of Advanced Technology & Engineering Research, Volume 4, Issue 1, Jan 2014.
6. Rajat Gupta, Sukanta Roy, Agnimitra Biswas, " CFD Analysis Airfoil Shaped Three Bladed H-Darreus Rotor", Proceedings of the 37th National & 4th International Conference on Fluid Mechanics and Fluid Power, December 16-18, 2010, IIT Madras, Chennai, India.
7. Rajat Gupta, Sukanta Roy, Agnimitra Biswas, "CFD analysis of a twisted airfoil shaped two-bladed H-Darrieus rotor made from fibreglass

reinforced plastic” International journal of ENERGY and ENVIRONMENT, Volume 1, Issue 6, 2010 pp.953-968.

8. S.M. Rassoulinejad-Mousavi, M. Jamil and M. Layeghi “Experimental Study of a Combined Three Bucket H-Rotor with Savonius Wind Turbine” World Applied Sciences Journal 28(2):205-211, 2013.
9. T.Letcher, “Small Scale Wind Turbines for Low Wind Speeds’.